

Near- T_c second-harmonic emission in high-density bulk MgB_2 at microwave frequency

A. Agliolo Gallitto¹, G. Bonsignore¹, G. Giunchi², and M. Li Vigni¹

¹ CNISM and Dipartimento di Scienze Fisiche e Astronomiche, Università di Palermo, Via Archirafi 36, I-90123 Palermo (Italy)

² EDISON S.p.A., Divisione Ricerca & Sviluppo, Via U. Bassi 2, I-20159 Milano (Italy)

the date of receipt and acceptance should be inserted later

Abstract. We discuss the microwave second-harmonic generation in high-density bulk MgB_2 , prepared by the reactive liquid Mg infiltration technology. The intensity of the harmonic signal has been investigated as a function of temperature and amplitudes of the DC and microwave magnetic fields. The results are discussed in the framework of a phenomenological theory, based on the two-fluid model, which assumes that both the microwave and static magnetic fields, penetrating in the surface layers of the sample, weakly perturb the partial concentrations of the normal and superconducting fluids. We show that, in order to account for the experimental results, it is essential to suppose that in MgB_2 the densities of the normal and condensed fluids linearly depend on the temperature.

PACS. 74.20.De Phenomenological theories (two-fluid, Ginzburg-Landau, etc.) – 74.25.Nf Response to electromagnetic fields (nuclear magnetic resonance, surface impedance, etc.) – 74.70.Ad Metals; alloys and binary compounds (including A15, MgB_2 , etc.)

1 Introduction

Investigation of the nonlinear microwave response of superconductors is of great interest for both fundamental and applicative aspects. From the basic point of view, it allows determining the electron-phonon scattering time [1, 2], the temperature dependence of the condensed and normal fluids [3, 4] and checking the presence of weak links in the sample [5, 6, 7, 8]. From the technological point of view, it is well known that the occurrence of nonlinear effects at high input-power levels limits the application of superconductors in passive microwave (mw) devices, while it has important implications in active devices [9, 10]. For these reasons, it is of importance estimating the mw current and field intensities at which nonlinear effects are significant and recognizing the mechanisms responsible for the nonlinearity at high frequencies.

Since the discovery of superconductivity in magnesium diboride, the scientific world has devoted large attention to this superconductor because of its peculiar properties, related to the two-gap structure of the electronic states, as well as its potential in technological applications [11, 12, 13]. It has been shown that the presence of the two gaps affects several properties of the MgB_2 superconductor, such as the fluxon structure [14, 15] and the temperature dependencies of the specific heat [16], critical fields [17, 18], condensed-fluid density [19, 20]. The advantages of using MgB_2 for technological applications are the simple crystal structure, the malleability and ductility, due to the metallic nature, the relatively high critical temperature,

the large coherence length, which makes the materials less susceptible to structural defects like grain boundaries [11, 21, 22]. One of the main effects of the nonlinear electromagnetic response of superconductors is the emission of signals at harmonic frequencies of the driving field [23]. Previous studies carried out in some bulk MgB_2 samples have shown that the microwave harmonic emission is significant in the whole range of temperatures below T_c and exhibits an enhanced peak at temperatures close to T_c [24, 25]. It has been shown that the harmonic emission at low temperatures is related to processes occurring in weak links, while a different mechanism is responsible for the near- T_c peak [24]. Furthermore, measurements of second-harmonic (SH) signal at DC magnetic fields smaller than the lower critical field, have shown that the SH signal due to weak links strongly depends on the specific properties of the sample [24, 26].

Recently, we have investigated the mw SH emission in three bulk samples of MgB_2 obtained by reactive infiltration of liquid Mg in powdered B preforms [27], which are characterized by different mean size of the grains (100, 40, 1 μm). We have shown that the intensity of the low-field and low- T SH signal strongly depends on the size of grains and, in particular, that the sample with the smallest grain size does not exhibit detectable low- T SH signal, proving that in such sample the nonlinear processes in weak links are not enough effective in the mw SH generation [26]. In this paper, we investigate the SH emission at temperatures close to T_c in the sample with grain mean size

of $\approx 1 \mu\text{m}$. The investigation is carried out at low magnetic fields, where nonlinear effects arising from motion of Abrikosov fluxons do not play a significant role in the harmonic emission. The results are discussed in the framework of a phenomenological theory, based on the two-fluid model, which assumes that both the mw and static magnetic fields, which penetrate in the surface layers of the sample, weakly perturb the partial concentrations of the normal and superconducting fluids [3,4]. We show that the results expected from this model satisfactorily account for the experimental data if a linear temperature dependence of the normal and condensed fluid densities is supposed.

2 Experimental Apparatus and Sample

The investigated MgB₂ sample was prepared by reactive liquid Mg infiltration technology [27]. Micron size amorphous boron powder (Grade I, 98% purity, Stark H.C., Germany) and pure liquid magnesium are inserted in a stainless steel container, with a weight ratio Mg/B over the stoichiometric value (≈ 0.55); the container was sealed by conventional tungsten inert gas welding procedure, with some air trapped inside the B powder; a thermal annealing at 900 °C for 30 min was performed. It has been shown that MgB₂ samples produced in this way have a density of 2.40 g/cm³ and consists predominantly of 1-micron size grains, although larger grains, of a few microns in size, are also present [28]. From the final product, we have extracted a sample of approximate dimensions $2 \times 3 \times 0.5 \text{ mm}^3$, whose largest faces have been mechanically polished to obtain very smooth surfaces.

The sample has been previously characterized by measuring the AC susceptibility at 100 kHz. From these measurements we have found that the transition can be described by a Gaussian distribution function of T_c , centered at $T_{c0} = 38.5 \text{ K}$ with $\sigma_{T_c} = 0.2 \text{ K}$. Furthermore, we have determined the lower and upper critical fields; in the range of temperatures of about 5 K below T_c , the critical fields show linear temperature dependence with $dH_{c2}/dT \approx 1.5 \text{ kOe/K}$ and $dH_{c1}/dT \approx 6.5 \text{ Oe/K}$.

In order to detect the SH signal, the sample is placed in a bimodal cavity, resonating at the two angular frequencies ω and 2ω , with $\omega/2\pi \approx 3 \text{ GHz}$, in a region in which the mw magnetic fields $\mathbf{H}(\omega)$ and $\mathbf{H}(2\omega)$ are maximal and parallel to each other. The ω -mode of the cavity is fed by a train of mw pulses, with pulse width 5 μs , pulse repetition rate 200 Hz, maximum peak power $\sim 50 \text{ W}$. The SH signal radiated by the sample is detected by a superheterodyne receiver. The cavity is placed between the poles of an electromagnet that generates DC magnetic fields up to $\approx 10 \text{ kOe}$; two additional coils, externally fed, allow reducing the residual field within 0.1 Oe and working at low magnetic fields. All the measurements have been performed with $\mathbf{H}_0 \parallel \mathbf{H}(\omega) \parallel \mathbf{H}(2\omega)$. The experimental apparatus is described in more details in Ref. [29].

3 Experimental Results

The SH emission has been investigated as a function of the temperature, DC magnetic field and input power level. In order to disregard SH signals due to nonlinear fluxon dynamics, the attention has been devoted to the SH response at low external fields. Before any measurement was performed, the sample was zero-field cooled (ZFC) down to a desired temperature value and then the magnetic field was applied.

Fig. 1 shows the SH signal intensity as a function of the temperature in the MgB₂ sample, at different values of the DC magnetic field. The SH emission is visible, with our experimental sensibility, only in a restrict range of temperatures below T_c (the dashed line indicates the noise level). The SH-*vs.*- T curves exhibit a peak just below T_c ; on increasing H_0 , the peak broadens and its maximum shifts towards lower temperatures.

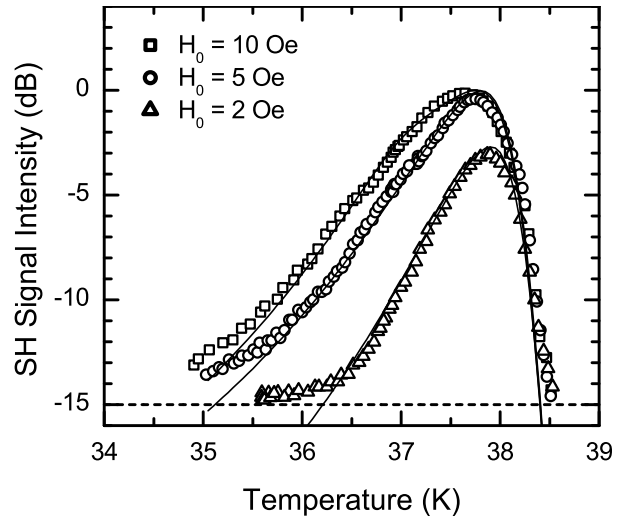


Fig. 1. SH signal intensity as a function of the temperature in the MgB₂ sample, for $H_0 = 10, 5, 2 \text{ Oe}$ as displayed from the top. Input peak power $\approx 30 \text{ dBm}$; the dashed line indicates the noise level that corresponds to $\approx -75 \text{ dBm}$. The curves are normalized to the maximal intensity of the SH signal detected at $H_0 = 10 \text{ Oe}$. The continuous lines have been obtained with the model discussed in the next section, using $\lambda_0/\delta_0 = 0.11$, $\alpha_0 = 2 \times 10^{-3} \text{ Oe}^{-1}$, $\alpha_1 H_1 = 8 \times 10^{-3}$.

Fig. 2 shows the SH signal intensity as a function of the DC magnetic field, at the two temperatures $T = 37.6 \text{ K}$ and $T = 36.7 \text{ K}$. The results have been obtained in the ZFC sample on increasing H_0 for the first time. As expected from symmetry considerations, the SH signal is zero at $H_0 = 0$; on increasing the field it rapidly increases, exhibiting a wide maximum at fields of few Oe. Both the slope of the SH-*vs.*- H_0 curves at $H_0 = 0$ and the position of the maximum depend on the temperature.

By sweeping the magnetic field from zero up to a certain value, H_{max} , and back, the SH signal shows a hysteretic behavior when H_{max} reaches a threshold value that depends on temperature. Fig. 3 shows the field dependence

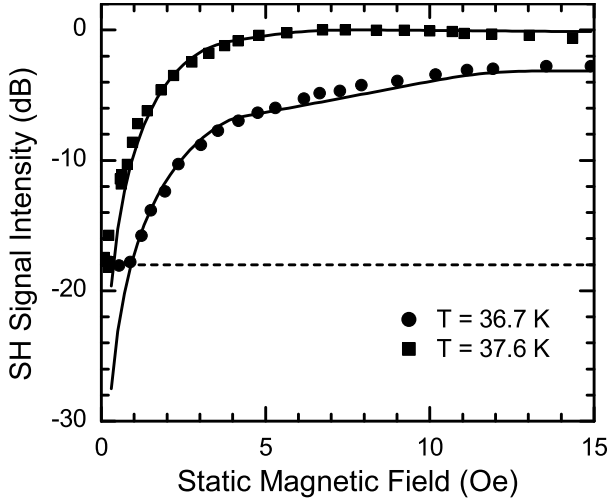


Fig. 2. SH signal intensity as a function of the static magnetic field, for $T = 37.6$ K and $T = 36.7$ K, as displayed from the top. Input peak power ≈ 30 dBm. The curves are normalized to the maximal intensity of the SH signal detected at $T = 37.6$ K. The dashed line indicates the noise level. The continuous lines have been obtained by the model discussed in the next section, using the same values of the parameters of Fig. 1.

of the signal obtained sweeping H_0 in the range ± 15 Oe, for $T = 37.6$ K. The presence of a magnetic hysteresis, as well as the observation of a noticeable SH signal at $H_0 = 0$, in the decreasing-field branch of the curve, suggest that trapped flux is present in the sample. So, we deduce that, even at temperatures near T_c , a critical state of the fluxon lattice develops. It is worth to remark that, on further increasing the DC magnetic field, the intensity of the SH signal decreases and, eventually, goes to zero when H_0 reaches the value of the upper critical field.

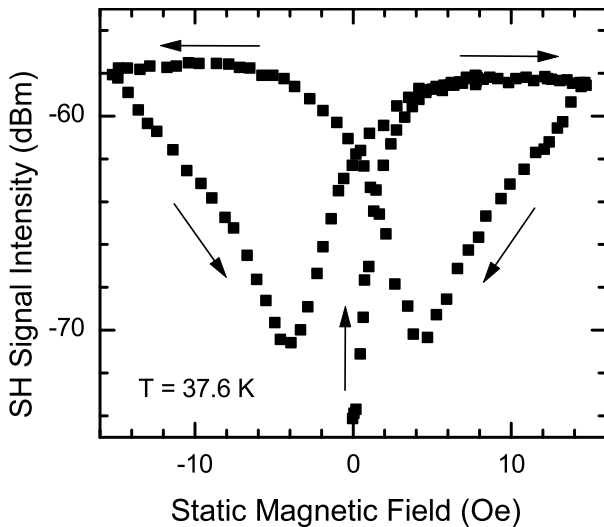


Fig. 3. SH signal intensity as a function of the static magnetic field, obtained sweeping H_0 in the range ± 15 Oe. Input peak power ≈ 30 dBm.

In Fig. 4 we report the power dependence of the SH signal at $H_0 = 2$ Oe, for two different values of the temperature. As one can see, the power dependence of the SH signal cannot be described by a mere n -order power law, indeed the slope of the SH-*vs.*- P_{in} line is not constant in the range of power levels investigated; in particular, at the investigated power levels the input-power dependence of the SH signal is less than quadratic.

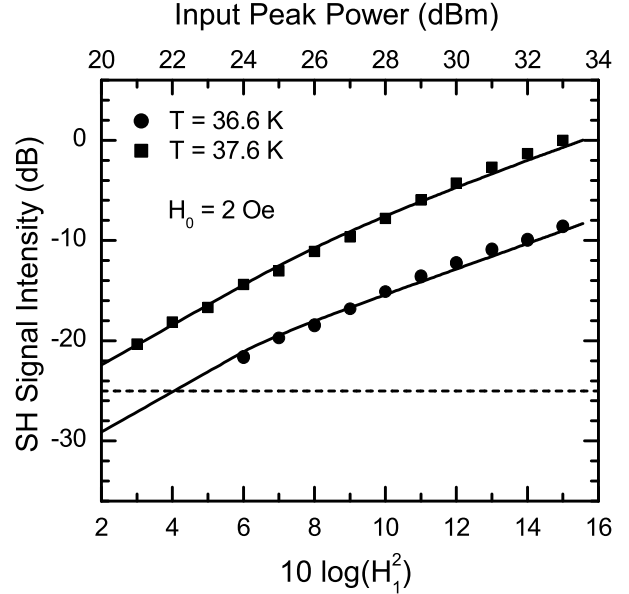


Fig. 4. SH signal intensity as a function of the input peak power for $H_0 = 2$ Oe and two different values of the temperature. The continuous lines have been obtained by the model discussed in the next section, using $\lambda_0/\delta_0 = 0.11$, $\alpha_1 = \alpha_0 = 2 \times 10^{-3} \text{Oe}^{-1}$. The dashed line indicates the noise level.

4 The Model

The nonlinear electromagnetic response has been investigated in conventional as well as in high- T_c superconductors [23]. Several mechanisms responsible for the harmonic emission have been recognized; their effectiveness depends on the temperature, DC magnetic field and type of superconductor. At DC fields smaller than the lower critical field, the harmonic emission at $T \ll T_c$ has been ascribed to nonlinear processes occurring in weak links [5, 6, 7], while at temperatures close to T_c it has been ascribed to modulation of the order parameter induced by the mw magnetic field [1, 3, 4, 6, 30].

Recently, we have investigated bulk MgB₂ samples prepared by different methods and in all of them we have detected a near- T_c peak in the SH emission; however, in most of them the peak mingles with the low- T signal [24]. As it has already been mentioned, the sample here investigated does not exhibit detectable SH emission at low fields and low temperatures, showing that the grain boundaries are not enough effective to give rise SH emission related to

processes occurring in weak links. This finding ensures the high sample quality and allows investigating the mechanism responsible for the harmonic emission near T_c in the MgB₂ superconductor.

Nonlinear emission at temperatures close to T_c is expected in the framework of several models, some work in the weak-coupling limit [2,31,32], others in the strong-coupling limit [30], others in the framework of the two-fluid model [3,4,6]. In all of them, the harmonic emission originates from the time variation of the order parameter induced by the em field.

From the models reported in Refs. [2,30,31,32], the input power dependence of the n th-harmonic signal is expected to follow an n -order power law. As it is shown in Fig. 3, we have observed a less than quadratic power dependence of the SH signal intensity; furthermore, the results reported in Ref. [25] show a less than cubic power dependence of the near- T_c third-harmonic signal in MgB₂. So, these models cannot justify the near- T_c harmonic emission in MgB₂.

Results of second and third harmonic emission near T_c by high- T_c superconductors have been justified quite well in the framework of the two-fluid model, with the additional hypothesis that both the mw and the DC magnetic fields, penetrating the sample in the surface layers, linearly perturb the partial concentrations of the normal and condensed fluids [3]. Since the processes occur in the surface layer of the order of the field penetration depth, they are effective only at temperatures close to T_c , where the energy gap is not large and the penetration depth is of maximal extent. The model has been discussed for the first time by Ciccarello *et al.* [3] to account for the experimental data of third-harmonic emission by YBa₂Cu₃O₇ (YBCO) single crystals in the absence of DC magnetic fields. Successively, it has been generalized to take into account the effect of the DC magnetic field and, further, justify the SH generation [4,6]. The model is valid in the limit of strong coupling, in which the approach of the two-fluid model can be reasonably used [33]. It has been shown that the model accounts very well for the results obtained in high- T_c superconductors in the Meissner state and qualitatively those obtained in the mixed state [4]. So, although it has been shown that the mechanism contributes to the harmonic emission also in the mixed state, others processes, related to the presence and motion of fluxons, may contribute to the nonlinear mw response of superconductors in the mixed state [34,35].

Since the near- T_c SH signal radiated by MgB₂ shows some peculiarities similar to those observed in YBCO and Ba_{0.6}K_{0.4}BiO₃ (BKBO) crystals [4,6], such as the input power dependence and the broadening of the peak on increasing H_0 , one can reasonably hypothesize that in these superconductors the mechanism responsible for the near- T_c SH emission is the same. However, few differences have to be mentioned: the SH emission is more enhanced in YBCO than in MgB₂ (at least one order of magnitude); the near- T_c peak is narrower in YBCO ($\sim T_c/30$) than in MgB₂ ($\sim T_c/10$); while in YBCO and BKBO the peak width, as well as the position of the maximum, depend

on the input power, these effects have not been detected in MgB₂. In the following of this section, we describe the model.

Coffey and Clem [36] have elaborated a comprehensive theory for the electromagnetic response of type-II superconductors in the framework of the two-fluid model of the superconductivity. It has been shown that the em field is characterized by a complex penetration depth

$$\tilde{\lambda}^2 = \frac{\lambda^2 + \delta_v^2}{1 - 2i\lambda^2/\delta^2}, \quad (1)$$

where

$$\lambda = \frac{\lambda_0}{\sqrt{(1 - w_0)(1 - B_0/H_{c2})}}, \quad (2)$$

$$\delta = \frac{\delta_0}{\sqrt{1 - (1 - w_0)(1 - B_0/H_{c2})}}. \quad (3)$$

In Eqs. (2) and (3), λ_0 is the London penetration depth at $T = 0$; $\delta_0 = (c^2/2\pi\omega\sigma_0)^{1/2}$ is the normal skin depth at $T = T_c$; w_0 and $1 - w_0$ are the fractions of normal and superconducting electrons at $H_0 = 0$, in the Gorter and Casimir two-fluid model $w_0 = (T/T_c)^4$. In Eq. (1), δ_v is the effective complex skin depth arising from the vortex motion. At mw frequencies and at temperatures close to T_c it is reasonable to assume that vortices move in the flux-flow regime; in this case, using the expression of the viscous-drag coefficient given by Bardeen and Stephen [37], it results $\delta_v^2 = 2\delta_0 B_0/B_{c2}(T)$, where B_0 is the magnetic induction due to the presence of fluxons.

For a sample of thickness D much greater than the characteristic penetration depths, the mw magnetic induction averaged over the volume of the crystal is

$$\langle B(t) \rangle = \frac{-H_1}{D} [\Im(\tilde{\lambda}) \cos \omega t + \Re(\tilde{\lambda}) \sin \omega t], \quad (4)$$

where H_1 is the amplitude of the mw field.

The Fourier coefficients of $\langle B(t) \rangle$ are given by

$$a_n = \frac{1}{\pi} \int_0^{2\pi} \langle B(t) \rangle \cos(n\omega t) d(\omega t), \quad (5)$$

$$b_n = \frac{1}{\pi} \int_0^{2\pi} \langle B(t) \rangle \sin(n\omega t) d(\omega t). \quad (6)$$

From a_n and b_n one can calculate the induced magnetization oscillating at $n\omega$ and, eventually, the intensity of the n th-harmonic signal.

The magnetic induction obtained using expressions (1)-(3) does not contain harmonic Fourier components because all the equations involved up to now are linear. Nonlinearity comes out on assuming that the mw field, penetrating the surface layers of the sample, modulates the partial concentrations of the normal and superconducting fluids [3].

In the Meissner state, also the DC magnetic field penetrates in the surface layers of the sample and it can perturb the partial concentration of the two fluids. On the

other hand, though we have performed measurements at low magnetic fields ($H_0 \sim 10$ Oe), at temperatures very close to T_c the sample goes in the mixed state; in this case, a part of the DC magnetic field penetrates as fluxons and the other is screened by the sample and is present in the surface layers. We suppose that both the mw and the screened DC magnetic field perturb the electron concentrations in a similar way. Following this idea, it has been set [4]

$$w(t, H_0) = w_0[1 + |\alpha_0 4\pi M + \alpha_1 H_1 \cos \omega t|], \quad (7)$$

where α_0 and α_1 are phenomenological parameters. By replacing w_0 in Eqs. (2) and (3) with $w(t, H_0)$ of Eq. (7), the em induction inside the sample is expected to have harmonic Fourier components, which can be calculated by using Eqs. (5) and (6). The power emitted by the sample at $n\omega$ is expected to be:

$$P_{n\omega} \propto a_n^2 + b_n^2. \quad (8)$$

5 Discussion

By using Eqs. (4-8) we have deduced the expected SH signal intensity. The integrals of Eqs. (5) and (6) cannot be solved analytically; they have been solved numerically with the proviso that $w(t, H_0) = 1$ whenever, because of the contribution of the perturbative terms in Eq. (7), its instantaneous value becomes greater than one. This condition is necessary since the concentration of normal electrons cannot exceed one and no modulation must occur when all electrons are in the normal state.

The calculations have been carried out in the following approximation: $|4\pi M|$ equal to H_0 for $H_0 \leq H_{c1}(T)$; $|4\pi M|$ linearly decreasing from $H_{c1}(T)$ to zero for $H_{c1}(T) \leq H_0 \leq H_{c2}(T)$.

The expected results depend on the ratio λ_0/δ_0 , the temperature dependence of w_0 and the parameters α_0 and α_1 . In particular, λ_0/δ_0 and the temperature dependence of w_0 determine the peak width, α_0 and α_1 the field and power dependence of the SH signal, respectively. Since the width of the near- T_c peak is most likely affected by the inhomogeneous broadening of the superconducting transition, we have calculated the averaged em induction (Eq. 4) taking into account the distribution of T_c over the sample. By using reasonable values of λ_0/δ_0 and the temperature dependence of w_0 expected from the Gorter and Casimir two-fluid model, we have obtained a near- T_c peak much narrower than the one experimentally observed. On the other hand, different authors [19,20,38,39] have shown that the temperature dependence of the field penetration depth in MgB₂ cannot be accounted for by either the Gorter and Casimir two-fluid model or the standard BCS theory. A linear temperature dependence of the condensed fluid density, in a wide range of temperature below T_c , has been reported, which has been justified in the framework of two-gap models for the MgB₂ superconductor [19,20].

Prompted by these considerations, we have calculated the averaged em induction over the sample, from Eq. (4),

supposing a linear temperature dependence of w_0 and using λ_0/δ_0 , α_0 and α_1 as parameters. The continuous lines of Figs. 1 and 2 show the temperature and field dependence of the SH signal, respectively, expected from the model. The best-fit curves have been obtained with $\lambda_0/\delta_0 = 0.11$, $\alpha_0 = 2 \times 10^{-3} \text{ Oe}^{-1}$ and $\alpha_1 H_1 = 8 \times 10^{-3}$. Since the amplitude of the mw magnetic field at which we have performed the measurements is about 4 Oe, we may estimate α_1 to be of the same order of α_0 . By using the same value of λ_0/δ_0 and setting $\alpha_1 = \alpha_0 = 2 \times 10^{-3} \text{ Oe}^{-1}$ we have obtained the continuous lines of Fig. 4 for the power dependence of the SH signal intensity. As one can see, the results expected from the model, hypothesizing that the normal and condensed fluid densities linearly depend on temperature, satisfactorily agree with the experimental data. We would remark that, by using the same values of the parameters before mentioned, we have found that, contrary to what occurs in other superconductors [3,4,6], the width of the SH near- T_c peak in MgB₂ is not appreciably affected by the amplitude of the microwave magnetic field. This finding, which agrees with the experimental observations, may be ascribed to the different values of the parameters used to fit the experimental data of MgB₂, with respect to those obtained in other superconductors.

Since $\lambda_0/\delta_0 = \sqrt{\omega\tau}/2$, by supposing λ_0 of the order of 100 nm we may estimate the scattering time of the normal electron to be $\tau \sim 10^{-12} \text{ s}$, which is of the same order of that reported in the literature for MgB₂ [40]. However, we would remark that we have assumed a linear temperature dependence of the condensed fluid density, which could be no longer valid at low temperatures; so, it is possible that the value of λ_0/δ_0 we found is not exactly equal to $\sqrt{\omega\tau}/2$.

The hysteretic behavior shown in Fig. 3 suggests that mechanisms related to trapped magnetic flux are effective. On the other hand, it is reasonable to hypothesize that at temperatures near T_c the sample goes in the mixed state for magnetic fields of the order of 10 Oe. The presence of the magnetic hysteresis suggests that a critical state of the fluxon lattice develops in the sample up to temperatures near T_c . Since the model here reported does not consider such effects, we did not fit these results. When the sample is in the critical state, the magnetic induction, B_0 , is different for applied magnetic field reached at increasing and decreasing field, causing a magnetic hysteresis in the SH signal. The sharp minima observed after the inversion of the field-sweep direction may be ascribed to the change of the critical current in the sample skin layer [30].

6 Conclusions

In conclusion, we have reported a set of experimental results on second harmonic generation at temperatures close to T_c in a bulk sample of MgB₂, prepared by the reactive liquid Mg infiltration technology. The SH signal has been investigated as a function of temperature and amplitudes of the DC and mw magnetic fields. The results have

been discussed in the framework of a phenomenological model previously elaborated to account for the nonlinear emission near T_c by YBCO and BKBO crystals. The model assumes that at temperatures close to T_c the mw and the DC fields, penetrating in the surface layers of the sample, perturb the partial concentrations of the normal and superconducting electrons. We have shown that, in order to account for the experimental results, it is essential to suppose that in MgB_2 the densities of the normal and condensed fluids linearly depend on the temperature. Such finding agrees with experimental results of the temperature dependence of the penetration depth reported in the literature, which have been justified in the framework of two-gap models for MgB_2 superconductor. We have shown that the enhanced nonlinear effects detected near T_c in MgB_2 have the same origin of those observed in YBCO and BKBO crystals. Though the superconductors have different nature, the description of the electromagnetic properties in terms of the two-fluid model seems to be appropriate. The different peculiarities of the near- T_c peak in the SH response, among the investigated superconductors, have to be ascribed to a different temperature dependence of the normal and condensed fluid densities.

Acknowledgements

The authors are very glad to thank E. Di Gennaro for his interest and helpful suggestions; G. Lapis and G. Napoli for technical assistance.

References

1. J. C. Amato and W. L. McLean, Phys. Rev. **36**, (1976) 930.
2. O. Entin-Wohlman, Phys. Rev. **B 18**, (1978) 4762.
3. I. Ciccarello, C. Fazio, M. Guccione, M. Li Vigni, and M. R. Trunin, Phys. Rev. **B 49**, (1994) 6280.
4. A. Agliolo Gallitto and M. Li Vigni, Physica **C 305**, (1998) 75.
5. I. Ciccarello, M. Guccione, and M. Li Vigni, Physica **C 161**, (1998) 39.
6. A. Agliolo Gallitto, M. Guccione, and M. Li Vigni, Physica **C 330**, (2000) 141.
7. C. D. Jeffries, Q. H. Lam, Y. Kim, L. C. Bourne, and A. Zettl, Phys. Rev. **B 37**, (1988) 9840.
8. L. Ji, R. H. Sohn, G. C. Spalding, C. J. Lobb, and M. Tinkham, Phys. Rev. **B 40**, (1989) 10936.
9. H. Weinstock and M. Nisenoff (eds.), *Microwave Superconductivity*, NATO Science Series, Series E: Applied Science - Vol. 375, Kluwer: Dordrecht 1999.
10. I. Vendik and O. Vendik, *High Temperature Superconductor Devices for Microwave Signal Processing* (Scalden Ltd, St. Petersburg, 1997).
11. Y. Bugoslavsky, G. K. Perkins, X. Qi, L. F. Cohen and A. D. Caplin, Nature **410** (2001) 563.
12. M. A. Hein, Proceedings of URSI-GA, Maastricht, August 2002. cond-mat/0207226.
13. E. W. Collings, M. D. Sunmption and T. Tajima, Supercond. Sci. Tech. **17** (2004) S595.
14. M. R. Eskildsen, M. Kugler, S. Tanaka, J. Jun, S. M. Kazakov, J. Karpinski and O. Fischer, Phys. Rev. Lett. **89**, (2002) 187003.
15. A. E. Koshelev and A. A. Golubov, Phys. Rev. Lett. **90**, (2003) 177002.
16. F. Bouquet, Y. Wang, I. Sheikin, T. Plackowski, A. Junod, S. Lee and S. Tajima, Phys. Rev. Lett. **89**, (2002) 257001.
17. M. S. Park, H. J. Kim, B. Kang and S.I. Lee, Supercond. Sci. Tech. **18**, (2005) 183.
18. V. H. Dao and M. E. Zhitomirsky, Eur. Phys. J. **B 44**, (2005) 183.
19. A. A. Golubov, A. Brinkman, O. V. Dolgov, J. Kortus and O. Jepsen, Phys. Rev. **B 66**, (2002) 054524.
20. C. P. Moca, Phys. Rev. **B 65**, (2002) 132509.
21. D. C. Larbalestier, L. D. Cooley, M. O. Rikel, A. A. Polyanski, J. Jiang, S. Patnalk, X. Y. Cal, D. M. Feldmann, A. Gurevich, A. A. Squitieri, M. T. Naus, C. B. Eom, E. E. Hellstrom, R. J. Cava, K. A. Regan, N. Rogado, M. A. Hayward, T. He, J. S. Slusky, P. Khalifah, K. Inumaru and M. Haas, Nature **410**, (2001) 186.
22. Neeraj Khare, D. P. Singh, A. K. Gupta, Shashawati Sen, D. K. Aswal, S. K. Gupta and L. C. Gupta, J. Appl. Phys. **97** (2005) 07613.
23. T. B. Samoilova, Supercond. Sci. Tech. **8**, (1995) 259, and references therein.
24. A. Agliolo Gallitto, G. Bonsignore and M. Li Vigni, Physica **C 432**, (2005) 306.
25. A. Agliolo Gallitto, G. Bonsignore and M. Li Vigni, Int. J. Mod. Phys. **B 17** (2003) 535.
26. A. Agliolo Gallitto, G. Bonsignore, G. Giunchi and M. Li Vigni, J. Phys.: Conf. Series, in press (cond-mat/0509201).
27. G. Giunchi, Int. J. Mod. Phys. **B 17** (2003) 453.
28. G. Giunchi, G. Ripamonti, S. Raineri, D. Botta, R. Gerbaldo and R. Quarantiello, Supercond. Sci. Tech. **17**, (2004) 583.
29. A. Agliolo Gallitto, G. Bonsignore, E. Di Gennaro, G. Giunchi, M. Li Vigni and P. Manfrinetti, cond-mat/0603648.
30. M. R. Trunin and G. I. Leviev, J. Phys. III France **2**, (1992) 355.
31. L. P. Gorkov and G. M. Eliashberg, Sov. Phys. JETP **27**, (1968) 328.
32. L. P. Gorkov and G. M. Eliashberg, Sov. Phys. JETP **28**, (1969) 1291.
33. V. L. Ginzburg and E. G. Maksimov, SPCT **5**, (1992) 1505.
34. M. W. Coffey, Phys. Rev. **B 46**, (1992) 567.
35. I. Ciccarello, C. Fazio, M. Guccione, and M. Li Vigni, Physica **C 159**, (1989) 769.
36. M. W. Coffey, J. R. Clem, Phys. Rev. **B 45**, (1992) 10527.
37. J. Bardeen, M. J. Stephen, Phys. Rev. **140**, (1965) A1197.
38. A. V. Pronin A. Pimenov, A. Loidl and S. I. Krasnosvobodtsev, Phys. Rev. Lett. **87**, (2001) 097003.
39. B. B. Jin, N. Klein, W. N. Kang, H. J. Kim, S. I. Lee, T. Dam, K. Maki, Phys. Rev. **B 66**, (2002) 104521.
40. Yu. A. Nefyodov, M. R. Trunin, A. F. Shevchun, D. V. Shovkun, N. N. Kolesnikov, M. P. Kulakov, A. Agliolo Gallitto and S. Fricano, Europhys. Lett. **58**, (2002) 422.